Formation of an intermediate 3 × 3 phase from Pb on Si(111) at high temperature

1999 J. Phys.: Condens. Matter 11 9925

(http://iopscience.iop.org/0953-8984/11/49/310)

J. Phys.: Condens. Matter **11** (1999) 9925–9932. Printed in the UK PII: S0953-8984(99)04489-6

Formation of an intermediate 3×3 phase from Pb on Si(111) at high temperature

A Petkova†, J Wollschläger, H L Günter and M Henzler

Institut für Festkörperphysik, Universität Hannover, Appelstrasse 2, D-30167 Hannover, Germany

E-mail: albena@fkp.uni-hannover.de (A Petkova)

Received 19 May 1999, in final form 19 August 1999

Abstract. Using high-resolution spot-profile-analysis low-energy electron diffraction (SPA-LEED) we have investigated low-coverage phases of Pb on Si(111) in the temperature range between 25 °C and 600 °C. After the annealing of 1/3 of a monolayer (ML) of Pb on Si(111) at 500 °C and cooling the sample down to room temperature, we observe a 3×3 phase beside the well known Pb/Si(111)$\sqrt{3} \times \sqrt{3}$R30° structure. The 3×3 phase is poorly ordered (domain size 20 Å–40 Å) compared to the $\sqrt{3} \times \sqrt{3}$ phase (domain size $\geqslant$1000 Å) as we conclude from profile analysis of the diffraction spots. The development of the 3×3 superstructure with increase of the annealing temperature was monitored and we observe a change of the domain size from 20 Å up to 40 Å upon annealing at 500 °C and 540 °C, respectively. After annealing at 580 °C the 3×3 phase has vanished and we detect only the $\sqrt{3} \times \sqrt{3}$ mosaic phase.

1. Introduction

Superstructures of metal films on semiconductor surfaces are of great interest and have been investigated by many physicists for many years. Pb on silicon and germanium substrates has been considered as a model system for the study of metal layer growth due to the inert nature of Pb and its insolubility in the bulk of Si and Ge [1]. Thus the Pb/Si system ought to provide a relatively simple interface to study. Furthermore, both Pb/Si(111) and Pb/Ge(111) have been proposed as candidates for studies of two-dimensional (2D) melting [2]. Considerable confusion and controversy exist, however, regarding the atomic structure, Pb coverages, annealing history and even the number of distinct phases for the Pb/Si(111) system (references [1–10]). This is, partly, due to the fact that Pb/Si(111) has a complex phase diagram above room temperature in which the already mentioned parameters coverage, temperature and annealing history play an important role.

The Pb/Si(111) system was first studied by Estrup and Morrison in 1964 using low-energy electron diffraction (LEED) [11]. They reported epitaxial growth of Pb on Si(111)7×7 in room temperature deposition, where the first adlayer is completed at $\frac{4}{3}$ ML (where 1 ML is defined as one Pb atom per surface Si atom, which is equal to 7.84×10^{14} Pb atoms cm^{-2}). After annealing, the 7×7 superstructure is destroyed and two different $\sqrt{3} \times \sqrt{3}$ phases at $\frac{1}{3}$ ML and $\frac{4}{3}$ ML, respectively, are observed. Saitoh *et al* [12] using low-energy ion scattering (LEIS) confirmed and extended these results. They concluded that Pb grows in the Stranski–Krastanov (SK) mode with the two-dimensional adlayer completed at about 1.3 ML. This knowledge was summarized

† Author to whom any correspondence should be addressed.

0953-8984/99/499925+08$30.00

in a phase diagram by Yaguchi *et al* [8] using reflection high-energy electron diffraction (RHEED). Subsequently, Le Lay and co-workers applied LEED, Auger spectroscopy (AES), thermal desorption spectroscopy (TDS) and ultraviolet photoemission spectroscopy (UPS) to this system [3, 4]. In contrast to the earlier results, they reported three different $\sqrt{3} \times \sqrt{3}$ phases at $\frac{1}{3}$, $\frac{2}{3}$ and $\frac{4}{3}$ ML and proposed a model with one, two and three Pb atoms per unit cell. The existence of these three $\sqrt{3} \times \sqrt{3}$ phases was confirmed by Quentel *et al* using *in situ* ellipsometry [5]. They reported that the first Pb adlayer is completed at 1 ML. Grey and co-workers [9, 10] studied the dense phases (near 1 ML) using x-ray diffraction. For room temperature deposition they proposed a close-packed 8×8 Pb layer on the Si(111)7×7 unit cell, while for an annealed film they proposed a 30°-rotated, close-packed, incommensurate (IC) model, corresponding to a saturation coverage of 1.3 ML. On the other hand Tanaka *et al* [13], using time-of-flight impact-collision ion scattering spectroscopy (TOF-ICISS), reported the completion of the first Pb adlayer at 1.5 ML in room temperature deposition. Furthermore, Ganz *et al* [6, 7] employed LEED, Rutherford backscattering spectroscopy (RBS), TDS and scanning tunnelling microscopy (STM) to study the growth and morphology of Pb/Si(111)7×7. Their results showed that Pb grows epitaxially up to 3 ML, at which point Pb islands start to form. On annealed samples at $\frac{1}{6}$ ML coverage, they found a new mosaic $\sqrt{3} \times \sqrt{3}$ phase which consists of alternating chains of Pb and Si adatoms at T_4 sites. For the IC phase, Ganz *et al* confirmed the 30°-rotated close-packed model proposed by Grey and co-workers, but they concluded that the coverage can range from 1 to 1.5 ML corresponding to a range of different Pb–Pb spacings.

Thus Pb adsorbed on a Si(111)7×7 surface shows various kinds of phase depending on coverage, temperature and annealing history. This leads to difficulties in proposing a complete phase diagram and in achieving a comprehensive understanding of the atomic structure and properties of the Pb layers on Si(111) substrates. Among the various phases, the $\sqrt{3} \times \sqrt{3}$ phase at $\frac{1}{3}$ ML has attracted considerable attention over the past few years because of its novel electronic properties and complicated atomic structure [14, 15].

In this work, we report on an intermediate 3×3 phase, which coexists with the Pb/Si(111)$\sqrt{3} \times \sqrt{3}$R30° phase. Using SPA-LEED, we observe this superstructure at room temperature after annealing in a small temperature range between 480 °C and 580 °C.

2. Experimental procedure

The experiments were performed in a standard ultrahigh-vacuum (UHV) chamber with a base pressure of 1×10^{-10} mbar. The UHV chamber is equipped with a SPA-LEED system, a sample transfer system, a mass spectrometer and an external electron gun for making *in situ* measurements during the Pb deposition. Clean vicinal Si(111) samples with 3° miscut were prepared by degassing at 600 °C for 12 hours and a short flash up to 1200 °C. After this preparation the diffraction spots do not show any splitting. Our calculations show that a sample with a miscut of 3° and monatomic steps must have 60 Å terraces, which will produce a splitting of the diffraction spots in the out-of-phase condition. But, as we mentioned above, we did not observe any splitting or extra diffraction spots. We concluded that the so-prepared Si samples have large terraces (width $\geqslant$1000 Å), larger than the instrumental resolution, and step bunches in between, separating these terraces. This cleaning procedure consistently yields high-quality Si(111)7×7 LEED patterns. The direction of the axis of intersection of the (111) plane and the surface one could not be determined from these measurements. The sample temperature was measured and controlled by an infrared pyrometer. Pb was evaporated from an effusion cell at a rate of 6×10^{-3} ML s^{-1}. The evaporator/sample distance was roughly

10 cm. The evaporation rate was controlled by a quartz microbalance close to the effusion cell. It was calibrated with a second quartz crystal microbalance at the sample position before starting the experiments. During the Pb deposition, the pressure was maintained at less than 2×10^{-9} mbar. In the 'one-step deposition', Pb was evaporated onto a clean Si(111)7 × 7 sample and then annealed. All SPA-LEED measurements reported in this work are performed at room temperature.

3. Results

Following deposition of 1 ML Pb on the Si(111)7 × 7 surface at room temperature (RT), we detect only changes of the intensity of the 7 × 7 superstructure spots, but no additional spots, i.e. Pb grows in the silicon 7 × 7 unit cell. The Si(111)7 × 7 unit cell is left unchanged. The Pb atoms occupy places above the rest atoms and between the Si adatoms [7, 16]. For this structure there are several models reported in the literature assuming different numbers of Pb atoms per Si(111)7 × 7 unit cell [7, 17]. But without exact determination of the Pb coverage, we cannot support any of them. We observe extra diffraction spots, shown in figure 1, after deposition of more than 2 ML of Pb. The positions of these spots, which we can determine with a high accuracy, correspond to the Pb bulk lattice constant $a_{\mathrm{Pb}} = 4.93 \pm 0.02$ Å. At this coverage, Pb island growth starts. Thus, we conclude that Pb grows on the Si(111) substrate in the Stranski–Krastanov mode in room temperature deposition (as other authors have reported previously [2,6,12]). Our measurements show that the first Pb layer is completed in the coverage range between 1 ML and 2 ML. For further statements, we need an exact determination of the Pb coverage, which cannot be achieved by means of quartz microbalance measurements alone. The accuracy of our experiments, however, shows that the value of 3 ML for the epitaxial Pb wetting layer on Si(111)7 × 7 measured by Ganz *et al* [6, 7] is too high and that the value of 1 ML given by Quentel *et al* [5] is too low.

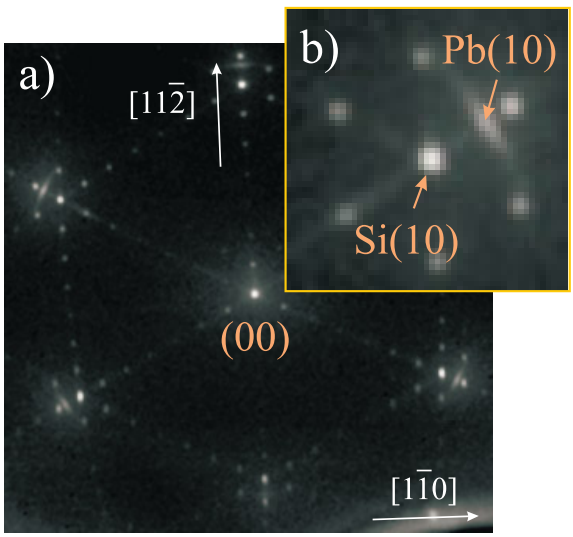

Figure 1. The diffraction pattern at 75.2 eV from 3 ML of Pb on the Si(111)7 × 7 surface evaporated at RT. The 7 × 7 superstructure spots are still visible. The Pb island spots are azimuthally broadened; due to ±2° rotational misorientation of the Pb(111) islands. (b) A magnified portion of the diffraction pattern close to the Si(10) spot.

A diffraction pattern from 3 ML of Pb deposited at RT on the Si(111)7 × 7 surface is shown in figure 1. We observe that the Pb(111) island spots are azimuthally broadened. A magnified portion of the two-dimensional diffraction pattern close to the Si(10) spot is shown in figure 1(b), where the 'banana'-shaped Pb(10) spot is clearly seen. This azimuthal broadening corresponds to a rotational misorientation of the Pb(111) islands within $\pm 2^\circ$ with respect to the crystallographic orientation of the supporting Si(111) substrate. This rotational alignment seems to be caused by a better fitting of the Pb(111) layer to the underlying Si(111) substrate. An alternative explanation of this rotation due to static distortion along the step edges (e.g. as for Xe on Cu(610) in reference [18]) is unlikely: the step edges have a much larger separation ($\geqslant$100 nm) than the Pb domains (40 nm, as we determined from the diffraction spot profile analysis). The 'banana' shape of the Pb spots (with doubled length for second-order spots) is not consistent with a wavy structure of the Pb islands. A wavy structure could anyway exist only close to the steps and cannot propagate over a distance of 40 nm. One-dimensional azimuthal scans along the extended Pb island spots are performed too. The spots are broadened, with a large full width at half-maximum (FWHM) of about 5%BZ (where '%BZ' means percentage of the Brillouin zone. 100%BZ corresponds to the normal spot distance of the Si(111) plane, $k = 2\pi/0.33$ nm^{-1}), but no extra intensity or splitting within the spot profiles is observed. This shows that there is no preferential angle by which the Pb(111) islands are rotated. All rotational angles in a range between -2° and $+2^\circ$ are possible, probably due to the different sizes of the Pb(111) islands.

After annealing of 1 ML of Pb deposited on Si(111)7 × 7 at room temperature to 480 °C for some minutes, we observe a phase transition to the $\sqrt{3} \times \sqrt{3}$R30° phase. The measured diffraction patterns show sharp superstructure spots. Figure 2(a) shows the diffraction pattern from the $\sqrt{3} \times \sqrt{3}$ phase obtained after cooling the sample to room temperature, with the normal and the first-order $\sqrt{3}$ superstructure spots.

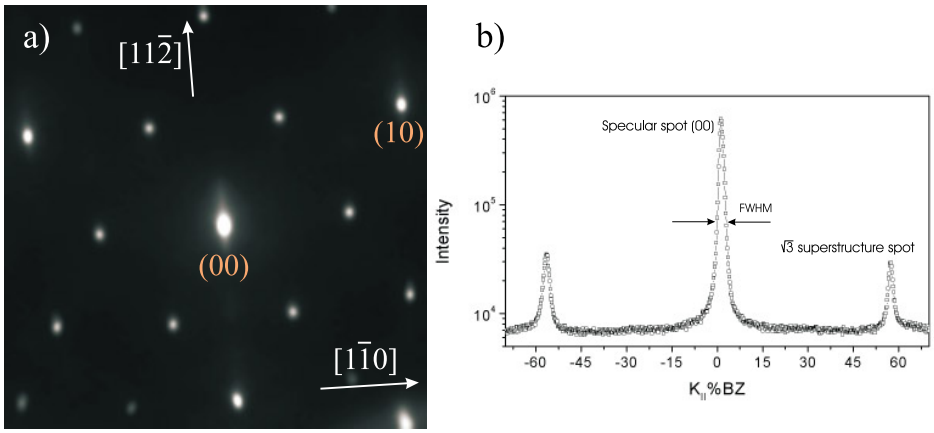

Figure 2. (a) The diffraction pattern at 64.4 eV (in-phase condition) from a $\sqrt{3} \times \sqrt{3}$R30° superstructure after annealing at 480 °C, measured at RT. (b) A one-dimensional scan along the [110] direction.

From the one-dimensional cut (figure 2(b)) it is easy to determine the FWHM of the diffraction spots. The specular (00) and the $\sqrt{3}$ spots are fitted with Lorentzian curves (with exponent $\frac{3}{2}$) because of the isotropic surface morphology. From the difference of their halfwidths (the FWHM of the $\sqrt{3}$ spot is 0.1%BZ to 0.4%BZ larger than the FWHM of the specular spot), we calculate the domain size of the $\sqrt{3} \times \sqrt{3}$ phase. The $\sqrt{3} \times \sqrt{3}$ superstructure

is well developed, with large domains between 1000 Å and 3000 Å.

Upon annealing this $\sqrt{3} \times \sqrt{3}$ phase to 500 °C, a weak ring of extra spots arises. The profiles of these spots were measured under different diffraction conditions. The positions of the spots do not change with the scattering phase $S \sim K_{\perp}$. Since the position is constant, we conclude that the spots are caused by a new superstructure. We can rule out the possibility that the spots are caused by facets, mosaics or atomic steps. This would lead to typical variation of the spot positions and the spot shapes during variation of the scattering phase. The measured spot positions show that the observed new superstructure is 3×3. By scanning along different crystallographic directions, the FWHMs of the superstructure spots are measured. They are rather broad (FWHM = 19%BZ) and the average domain size of the 3×3 phase is determined to be approximately 20 Å.

After annealing to 540 °C, the ring of 3×3 superstructure spots is more clearly seen (figure 3(a)). Additionally, higher-order spots become visible. Figure 3(b) shows a one-dimensional scan along the $[2\bar{1}1]$ direction, where the $(\frac{1}{3}0)$ and $(\frac{2}{3}0)$ spots are seen. The FWHM of the first-order superstructure spots decreases to 9%BZ. Thus, the domain size of this phase increases to 40 Å, i.e. the 3×3 superstructure is better developed at this annealing temperature. One can see (figure 3(a)) that some intensity is observed in the directions of the $\sqrt{3}$ spots ($[1\bar{1}0]$ directions), where there must be no spots or intensity. The first-order superstructure spots seem to form a ring, but this is due to the superposition of the broad 3×3 superstructure spots. This result is based on the procedure of fitting the diffraction spots $(\frac{1}{3}0)$ and $(0\frac{1}{3})$ in the $[11\bar{2}]$ direction, which shows that we can reproduce the experimental spot profiles using only two Gaussian curves for the fitting of the two spots (figure 3(c)). Because they are so extended, a 'bridge' is formed between them.

Upon annealing to 580 °C, the 3×3 superstructure vanishes and we observe a superposition

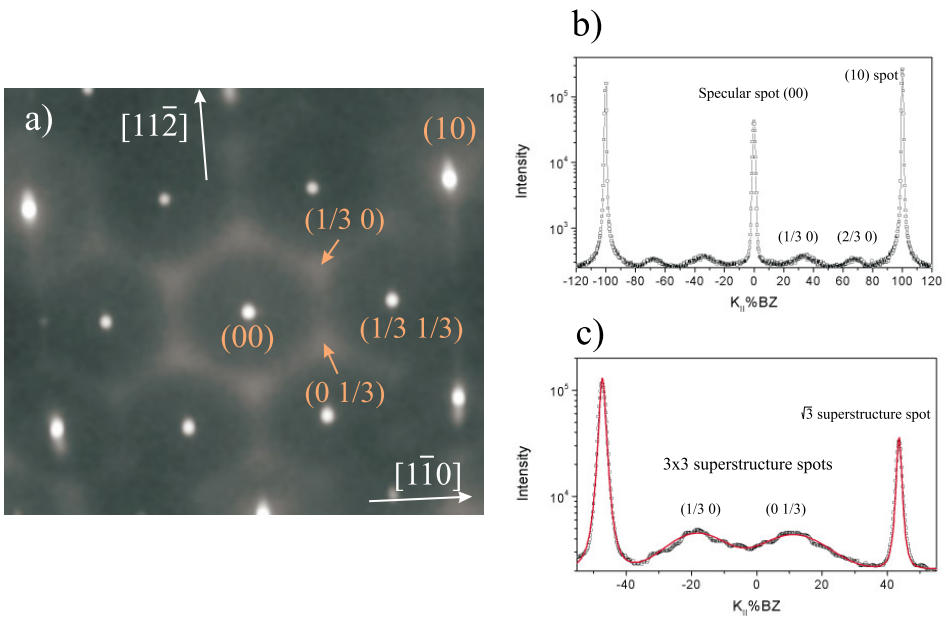

Figure 3. (a) The diffraction pattern at 64.4 eV from the mixture of 3×3 and $\sqrt{3} \times \sqrt{3}$R30° domains after annealing at 500 °C. (b) A one-dimensional cut along the $[2\bar{1}1]$ direction. (c) A one-dimensional cut along the $[11\bar{2}]$ direction.

of the $\sqrt{3} \times \sqrt{3}$ and 7×7 diffraction patterns. The structure with coexisting $\sqrt{3} \times \sqrt{3}$ and 7×7 superstructures is well known as the γ-$\sqrt{3} \times \sqrt{3}$ phase or $\sqrt{3} \times \sqrt{3}$ mosaic phase [6,19].

4. Discussion

In figure 4 we present a model for the observed 3×3 superstructure. The schematic diffraction pattern for this phase is shown in figure 4(a). The squares denote the fundamental spots, the dark circles the superstructure spots of the $\sqrt{3} \times \sqrt{3}$ phase and the big grey circles the superstructure spots of the 3×3 structure, additional to those of the $\sqrt{3} \times \sqrt{3}$ phase. As can be seen, the calculated and the observed diffraction patterns (figure 3(a)) are similar. But there remain some open questions which we want to discuss here. First, the observed diffraction pattern, presented in figure 3(a), could arise from any of three different surfaces: from a single 3×3 phase where some diffraction spots (one of them $(\frac{1}{3}\frac{1}{3})$ is marked on figure 3(a)) are identical with $\sqrt{3}$ spots; from a mixture of $\sqrt{3} \times \sqrt{3}$ and three 3×1 rotation domains; and from a mixture of 3×3 and $\sqrt{3} \times \sqrt{3}$ domains.

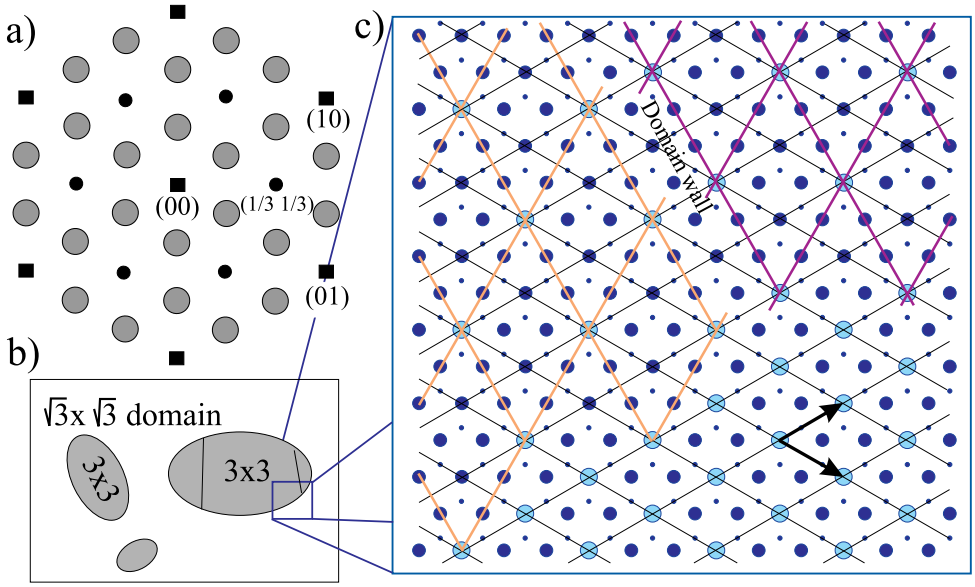

Figure 4. (a) The calculated diffraction pattern for the 3×3 superstructure. (b), (c) The real-space model for the 3×3 superstructure. Black points denote the second Si layer, black circles denote the first Si layer and big grey circles denote the Pb atoms.

We start with the $\sqrt{3} \times \sqrt{3}$R30° structure (figure 2(a)). The 3×3 diffraction pattern is observed after annealing over the temperature range between 500 °C and 580 °C. Upon annealing to 580 °C the 3×3 superstructure spots disappear, the 3×3 phase vanishes and the $\sqrt{3} \times \sqrt{3}$ mosaic phase is observed. Thus, the 3×3 phase exists between two different $\sqrt{3} \times \sqrt{3}$ phases. We conclude that there is no evidence that the $\sqrt{3} \times \sqrt{3}$ phase vanishes between these two $\sqrt{3}$ phases in the intermediate range where the 3×3 superstructure forms. This would mean that the Pb atoms move back to the $\sqrt{3} \times \sqrt{3}$ unit cells after the disappearance of the 3×3 phase. So we assume that the $\sqrt{3} \times \sqrt{3}$ phase exists over the entire temperature range between 480 °C and 580 °C. The first candidate, the single 3×3 phase with small domain size, can be ruled out since the superstructure spots at $\sqrt{3}$ positions are sharp.

The observed diffraction pattern could be produced from a mixture of $\sqrt{3} \times \sqrt{3}$ and three 3×1 rotational domains. To get a 3×1 structure it is necessary to move Pb atoms from their $\sqrt{3}$ positions without evaporation of Pb. But a lot of experimental evidence exists indicating that at these high annealing temperatures Pb evaporates from the Si substrate. First, from the literature, it is known that the $\sqrt{3} \times \sqrt{3}$ structure exists at $\frac{1}{3}$ ML coverage [7,16]. On increasing the annealing temperature, Pb atoms evaporate partially, so at $\frac{1}{6}$ ML coverage the $\sqrt{3} \times \sqrt{3}$ mosaic phase appears [6, 19]. So we conclude that the observed structure transition must be accompanied by dilution of the Pb density on the Si(111) surface. From these considerations, we conclude that the observed structure can only be explained by the coexistence of large $\sqrt{3} \times \sqrt{3}$ domains and small 3×3 domains.

Possible positions of the Pb atoms in real space are presented in figure 4(c). We cannot reach an unambiguous conclusion as to where exactly the Pb atoms are placed or how many Pb atoms are in the 3×3 unit cell. Figure 4(c) shows our model with one Pb atom per 3×3 unit cell. The inverse structure with two Pb atoms per unit cell is also possible. Finally, we cannot even exclude a combination of these two possibilities with three Pb atoms at non-equivalent positions. As explained before, this last model, however, is very unlikely, since the formation of the 3×3 phase must be accompanied by the evaporation of Pb atoms. Scanning tunnelling microscopy (STM) measurements on this phase would be helpful in clarifying the structure of the 3×3 phase.

In figure 3(a) it is seen that the extra spots at $\sqrt{3} \times \sqrt{3}$ positions are extremely sharp, whereas the other extra spots of the 3×3 structure are rather diffuse. The domains of the 3×3 superstructure are small (approximately 40 Å). A mixture of small 3×3 domains and large $\sqrt{3} \times \sqrt{3}$ domains side by side would yield a shoulder around all $\sqrt{3}$ spots. Figure 3 clearly shows that this is not the case. Therefore the 3×3 domains cannot be arranged at random. The 3×3 structure may have nine different translational domains corresponding to nine substrate lattice vectors within the unit mesh. If out of the nine possibilities only the three vectors of the $\sqrt{3} \times \sqrt{3}$ structure within the 3×3 unit mesh are realized, all spots of the $\sqrt{3}$ positions should be sharp. Therefore the observed structure is fully explained by the 3×3 structure with small domains, which are correlated with domain walls with translation vectors of the $\sqrt{3}$ structure, as shown in figure 4(c).

Previously, the existence of 3×3 structures for different metal–semiconductor systems such as Sn/Ge(111) [20], Pb/Ge(111) [21], Pb/Si(111) [22] at temperatures below RT has been reported. This structure was never observed at room temperature, but this may be due to the lack of sensitivity of the experimental methods employed. Using SPA-LEED, we are extremely sensitive to low-intensity diffraction patterns. Thus even poorly developed superstructures, which produce broad diffraction spots with large FWHMs, can be detected.

5. Summary

Pb grows at room temperature in the Stranski–Krastanov mode. Our measurements show that the first Pb layer is completed in the coverage range between 1 ML and 2 ML—but we cannot give an exact value without further measurements. We observed, after the completion of the first Pb layer, island growth. These Pb islands are rotationally misoriented within $\pm 2^\circ$ with respect to the underlying Si(111) substrate. This misorientation is not influenced by the substrate steps (the distance between them is $\geqslant$100 nm), while the Pb domains have an average size of 40 nm (as we determined from the radial FWHM of the Pb diffraction spots). This rotational alignment is probably due to the better fitting of the Pb(111) layer to the Si(111) substrate.

Furthermore, we observe a high-temperature 3×3 superstructure, which coexists with

the $\sqrt{3} \times \sqrt{3}$ structure over a small temperature range between 480 °C and 580 °C. The development of the 3×3 phase with increase of the annealing temperature was monitored. Using SPA-LEED, we observed a change of the domain size from 20 Å up to 40 Å upon annealing at between 500 °C and 540 °C, respectively. We proposed a model for the observed structure. STM measurements for this phase would be helpful for clarifying the structure of the 3×3 phase and checking the proposed model.

Careful superstructure studies like the present one elucidate the ordering processes which are decisive for the description of other properties such as the 2D electronic properties of metallic adlayers.

Acknowledgment

This research was supported by the Gratuiertenkolleg Universität Hannover and the Deutsche Forschungsgemeinschaft.

References

[1] Le Lay G, Abraham M, Kahn A, Hricovini K and Bonnet J E 1991 *Phys. Scr.* T **35** 261
[2] Le Lay G 1997 *Growth and Properties of Ultrathin Epitaxial Layers* ed D A King and D P Woodruff (Amsterdam: Elsevier Science)
[3] Le Lay G, Hricovini K and Bonnet J E 1989 *Appl. Surf. Sci.* **41+42** 25
[4] Le Lay G, Peretti J, Hanbücken M and Yang W S 1988 *Surf. Sci.* **204** 57
[5] Quentel G, Gauch M and Degiovanni A 1988 *Surf. Sci.* **193** 212
[6] Ganz E, Xiong F, Hwang Ing-Shouh and Golovchenko J 1991 *Phys. Rev.* B **43** 7316
[7] Ganz E, Hwang Ing-Shouh, Xiong F, Theiss Silva K and Golovchenko J 1991 *Surf. Sci.* **257** 259
[8] Yaguchi H, Baba S and Kinbara A 1988 *Appl. Surf. Sci.* **33+34** 75
[9] Feidenhans'l R, Grey F, Nielsen M and Johnson R L 1990 *Kinetics of Ordering and Growth at Surfaces* ed M G Lagally (New York: Plenum) p 189
[10] Grey F, Feidenhans'l R, Nielsen M and Johnson R L 1989 *J. Physique Coll.* C7 181
[11] Estrup P J and Morrison J 1964 *Surf. Sci.* **2** 465
[12] Saitoh M, Oura K, Asano K, Shoji F and Hanawa T 1985 *Surf. Sci.* **154** 394
[13] Tanaka Y, Morishita H, Ryu J T, Katayama I and Oura K 1996 *Surf. Sci.* **363** 161
[14] Weitering H H, Ettema A R H F and Hibma T 1992 *Phys. Rev.* B **45** 9126
[15] Heslinga D R, Weitering H H, van der Werf D P, Klapwik T M and Hibma T 1990 *Phys. Rev.* B **64** 1589
[16] Hwang Ing-Shouh, Martinez R E, Liu Ch and Golovchenko J A 1995 *Surf. Sci.* **323** 241
[17] Wemmenhove M and Hibma T 1993 *Surf. Sci.* **287+288** 925
[18] Bardi U, Glachant A and Bienfait M 1980 *Surf. Sci.* **97** 137
[19] Gomez-Rodriguez J M, Veuillen J Y and Cinti R C 1997 *Surf. Sci.* **377–379** 45
[20] Le Lay G, Aristov V Yu, Bostöm O, Layet J M, Asensio M C, Avila J, Huttel Y and Cricenti A 1998 *Appl. Surf. Sci.* **123+124** 440
[21] Avila J, Mascaraque A, Michel E G and Asensio M C 1998 *Appl. Surf. Sci.* **123+124** 626
[22] Horikoshi K, Tong X, Nagao T and Hasegawa Sh 1999 at press